DETECTION OF INTERTURN FAULT IN THREE PHASE SQUIRREL CAGE INDUCTION MOTOR USING MAGNET

Nagarajan S.
Research Scholar
nagu_shola@yahoo.com
+919444177170

Rama S. Reedy
Professor
srr_victory@yahoo.com
+919840058140

Department of Electrical and Electronics Engineering, Jerusalem College of Engineering, Chennai, India

Abstract— *In Industry the predictive maintenance has become a strategic concept. Economic interest of on line diagnosis of faults in electric machines gave rise to various researches in that field. This paper presents the fault detection of three phase squirrel cage induction motor using finite element model of the machine. Accurate models of the machine under healthy and faulty conditions are developed using finite element method and the performance of the motor is examined.*

In this paper, the static two-dimensional analysis is done for stator inter turn fault. The machine parameters like flux linkage, flux density, stored magnetic energy are obtained for healthy and faulty motor. The results examined under various conditions are compared and the observations are presented.

Keywords— *inter-turn fault, Induction motor, ,flux linkage,magnetic energy, Finite Element.*

1. Introduction

Three phase induction motors have wide applications in various industries. It is recognized that a variety of faults can occur in these motors during normal operation such as rotor fault (broken bars or end ring), stator inter-turn fault, eccentricity fault and bearing fault. Hence early detection and diagnosis of such faults are very essential for the protection of induction motors against failures and permanent damages. A sudden motor failure may reduce productivity and may be catastrophic in an industrial system if undetected. In recent years, the problem of failures in large machines have become more significant, the desire to improve the reliability of the industrial drive systems has led to researches and developments in various countries to evaluate the cause and consequences of various fault conditions.

A variety of conditions monitoring techniques and signature analysis methods have been developed. An analytical approach based on the rotating field theory and coupled circuit is often used. Online fault diagnostic system increases industrial efficiency and reliability, these are usually simulated using FFT analysis. Other emerging commercial electromagnetic CAD packages like MagNet, EMTDC, Femta fe, Slim fe, Ansoft, etc., can be used for the fault detection of non-invasive methods. Finite element analysis, which is a computer based numerical technique, is used for calculation of the machine parameters like flux density, flux linkage, torque, induced electromagnetic field, etc., accurately. This analysis allows the effects of stator winding distribution, magnetic saturation and non-uniform current distributions to be considered simultaneously.

2. Literature Review

Transient Analysis of induction Motor Using Finite Element Analysis deals with transient performances which are predicted at the starting of the motor with no load, the operation of the motor with asymmetrical excitation of the stator and during turn to turn fault condition. The geometric dimension of induction motor is modeled in the finite element domain [1]. Diagnosis and Characterization of Effects of Broken Bars and Connectors in Squirrel-Cage Induction Motor by Time-Stepping Coupled Finite Element State Space Modeling Approach deals with the approach for diagnosis and characterization of the effects of rotor broken bars and connectors. The model is used to compute/predict the characteristic frequency components which are indicative of rotor bar and connector breakages [2].

On Line Diagnosis of Defaults on Squirrel Cage Motor Using FEM proposes an approach based on the signature of the global and external variables which are used to tackle problems of breaking bars and end ring. This allows a finer analysis by use of a finite element based simulation, better accuracy and simpler mode of detection [3]. Finite Element Analysis of Three Phase Induction Motors: Comparison of Two Different Approaches presents two different approaches that are used to analyze the motor fed by a symmetric three phase AC voltage

source. The first method is based on the equivalent circuit of the motor and the second method is based on the field solution. Both the approaches work with a 2D discretized domain [4]. Detection of Broken Bars in the Cage Rotor on an Induction Machine deals with broken bars detection using experimental set ups and compared with simulations done using finite element analysis. Computations were done using non-linear complex steady state technique [5].

Analysis and Diagnostics of Adjacent and Nonadjacent Broken-Rotor–Bar Faults in Squirrel-Cage Induction Machines describes how nonadjacent bar breakages result in the masking of the commonly used fault indices and other problems and the solutions to overcome these problems [6]. Designing Squirrel Cage Rotor Slots with High conductivity describes how deep bar and multiple cage effects are useful in design of induction machines. Casting copper in rotors of induction motor gives higher conductivity [7]. The Use of Finite Element Methods to Improve Techniques for the Early Detection of Faults in 3-Phase Induction Motors describes how commercial finite element packages may be used to simulate rotor faults and hence enhance the capability of practical condition monitoring schemes. Accurate models of the machine under faulted conditions are developed using both fixed mesh and time-stepping finite element packages [8].

Finite Element Analysis of Field Distribution and Characteristic Performance of Squirrel-Cage Induction Motor with Broken Bars deals with the foundation technique for the effects of broken bars fault in squirrel cage induction motor simulated using time stepping coupled with finite element technique [9]. Influence of Nonconsecutive Bar Breakages in Motor Current Signature Analysis for the Diagnosis of Rotor Faults in Induction Motors gives the analysis and simulations to investigate the influence that the number and location of faulty bars has on the traditional MCSA diagnosis procedure. The analysis is based on the fault current and space vector theory which provides a physical interpretation of the appearance of the left side band component under any double bar breakages [10]. The Use of the Wavelet Approximation Signal as a Tool for the Diagnosis of Rotor Bar Failures presents a study of an approximation signal resulting from the wavelet decomposition of the startup stator current. The presence of the left side band harmonic is used as evidence of the rotor failure in most diagnosis methods based on the analysis of the stator current. The diagnosis method proposed, consists of checking if the selected approximation signal fits well the characteristic shape of the left sideband harmonic evolution [11].

Induction Machine Broken-Bar Fault Diagnosis Using the Rotor Magnetic Field Space-Vector Orientation deals with a technique based on rotor magnetic field space vector orientation, presented to diagnose broken-bar faults in induction machine operating at steady state. The currents and voltages have swing-like pendulous oscillation in case of broken bars [12]. Induction Motor Analysis by Time-Stepping Techniques conveys that the equivalent circuit approach usually gives adequate predictions of torque and current but gives no information on flux distribution. This deficiency is overcome by numerical approach which uses 2D, nonlinear, time-stepping finite element method for excitation from a constant voltage source. Comparison of stator current for no load and other load conditions show good agreement with test values on a large induction motor [13].

Modeling of IM with Stator Winding Inter-turn Fault Validated by FEM deals with a dynamic model for induction motor with inter-turn winding fault. The model is validated by time stepping finite element analysis. The model is used for studying the machine behavior under fault conditions [14]. Calculation of Cage Induction Motor Equivalent Circuit Parameters using Finite Elements describes about the conventional equivalent circuit model to determine the equivalent circuit components for a three phase squirrel cage induction motor using finite element model. The use of minimal models leads to a fast execution time. The method uses separate finite element models for rotor and stator [15].The static two dimensional analysis done for stator inter turn fault and the results were compared with healthy motor[16].

The above literature use MATLAB for fault detection and modeling . In the present work, the fault analysis is done with a CAD package called MagNet, which is derived from the concept of magnetics.

3. Simulation of Healthy Induction Motor

A 415V, 50Hz, four-pole, 16HP squirrel cage three phase induction motor with 86 turns in each stator phase, 28 rotor bars and 36 stator slots with double layer winding is considered for simulation. The model is developed using Magnet simulation tool. The discretization of the entire geometry is shown in Fig. 1.

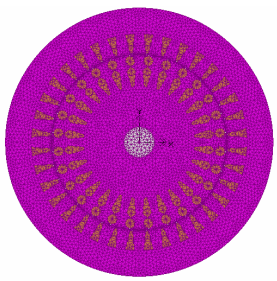

Fig. 1. Discretization of the model

A. Distribution of Magnetic Field and Flux

Inter-turn fault occurs due to the failure of insulation in the windings. Under the normal load conditions, the flux distribution in the fault region is distracted. Field and flux distribution plots under the normal load conditions for the case of healthy motor for no load, half load and full load conditions are shown in Fig. 2.

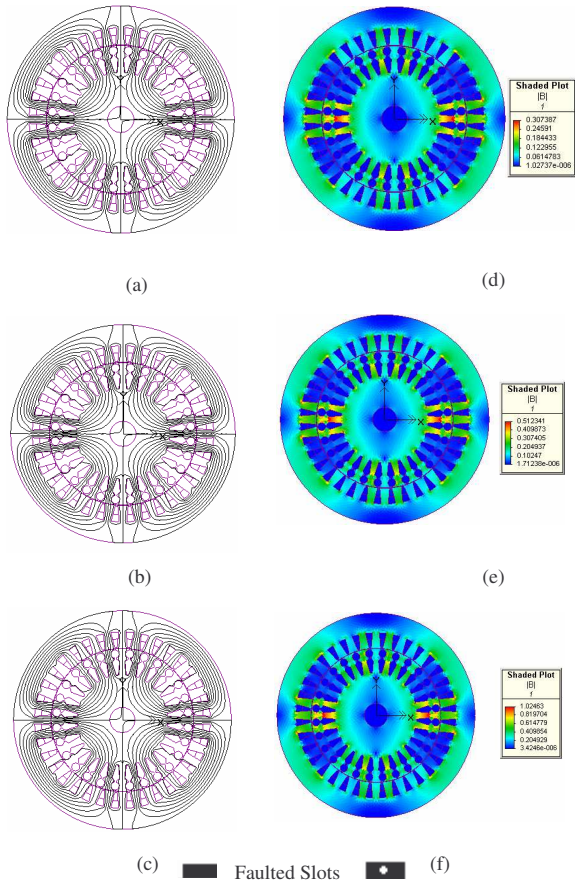

Fig. 2. Magnetic Field and Flux Distribution for healthy Conditions

Field Distribution under: (a) No Load; (b) Half Load; (c) Full Load

Flux Distribution under: (d) No Load; (e) Half Load; (f) Full Load

4. Simulation of Induction Motor with Stator Inter-Turn Fault

Inter-turn fault occurs due to the failure of insulation in the windings. Samples of field distribution and flux distribution plots for the case of faulty motor for no load, half load and full load conditions with 10% and 20% inter-turn short are shown in Fig. 3 & 4 respectively. It can be observed that the plots change their symmetry drastically when the percentage of inter turn faults in the stator slots increases. Table I shows the comparison of magnetic field energy for the faulty cases with the normal condition.

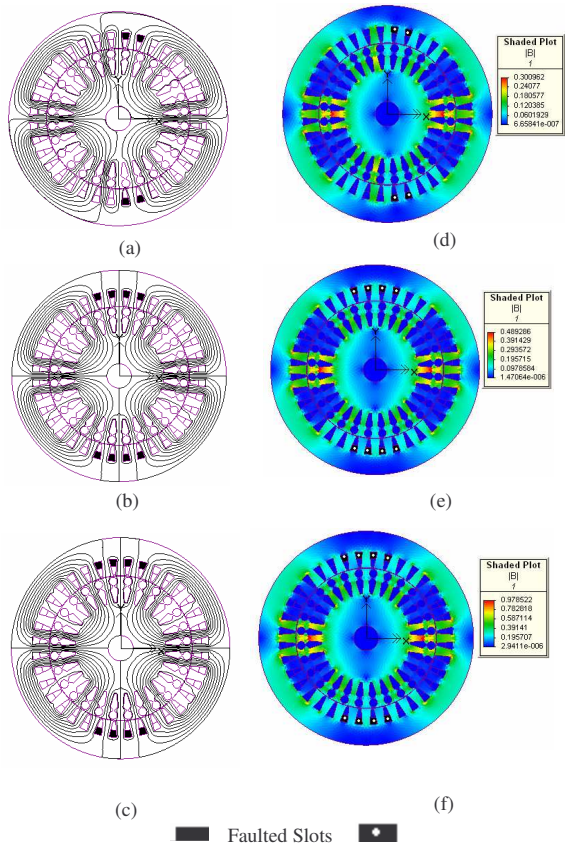

Fig. 3. Magnetic Field and Flux Distribution under 10% Inter-Turn Fault Conditions

Field Distribution under: (a) No Load; (b) Half Load; (c) Full Load

Flux Distribution under: (d) No Load; (e) Half Load; (f) Full Load

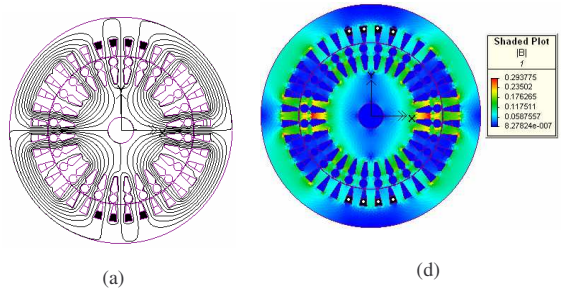

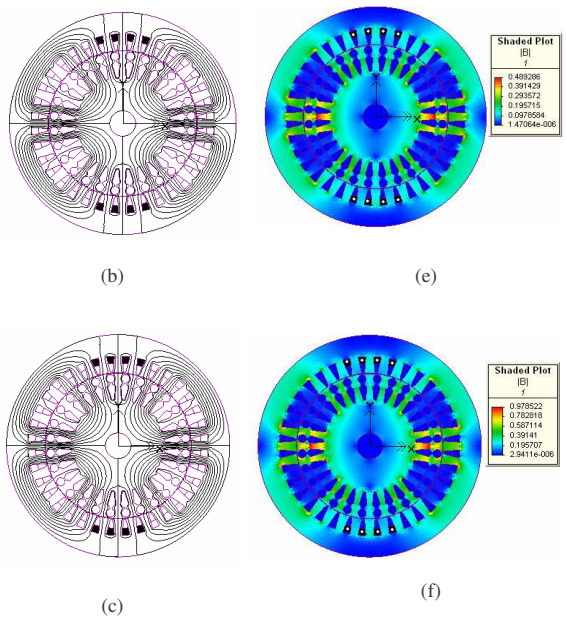

Fig. 4 Magnetic Field and Flux Distribution under 20% Inter-Turn Fault Conditions

Field Distribution under: (a) No Load; (b) Half Load; (c) Full Load

Flux Distribution under: (d) No Load; (e) Half Load; (f) Full Load

Table 1. Stored magnetic energy under various conditions

Condition		Stored Magnetic Energy (Joules)	Percentage Change (%)
No Load	Normal	0.000975	-
	10%Fault	0.000893	8.37
	20%Fault	0.000806	17.28
Half Load	Normal	0.002710	-
	10%Fault	0.002477	8.57
	20%Fault	0.002236	17.49
Full Load	Normal	0.010839	-
	10%Fault	0.009910	8.57
	20%Fault	0.008943	17.49
125% Load	Normal	0.016936	-
	10%Fault	0.015484	8.57
	20%Fault	0.013973	17.49
150% Load	Normal	0.024352	-
	10%Fault	0.022279	8.51
	20%Fault	0.020115	17.39

From Table 1, it can be observed that the stored magnetic energy decreases as the percentage of short in the stator slots increases from 10% to 20%,an increase in the energy is seen when load increases from no load to full load condition. The change in stored magnetic energy for 10% short is around 8%, for 20% short is around 17%. This analysis shows a decrease in the magnetic energy when the percentage of inter-turn short increases. Also the change is similar for all the load conditions and they are found with respect to the normal conditions in each case.

A. Field and Flux Profile in Rotor Core

Field and flux distribution in air-gap is evaluated with respect to the circumference which is shown in mm. The plots for no load, half load and full load conditions for healthy motor are shown in Fig. 5.

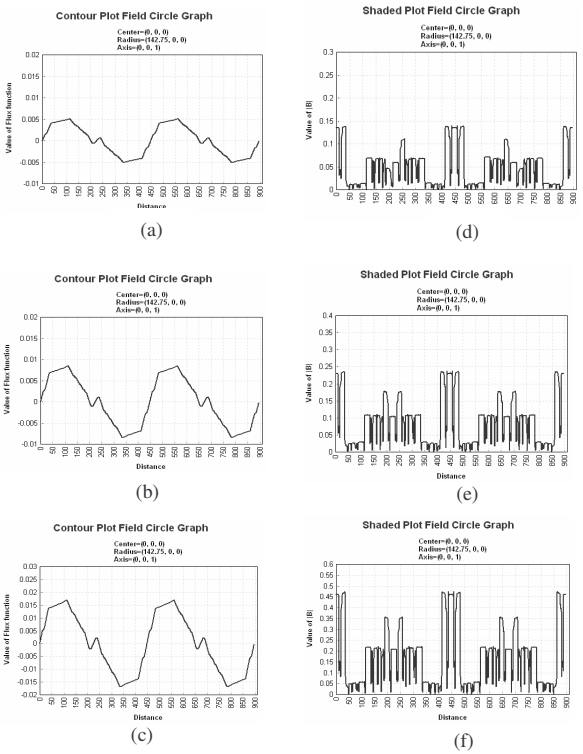

Fig. 5 Field and Flux Distribution in Air-Gap under Healthy Conditions

Field Distribution under: (a) No Load; (c) Half Load; (e) Full Load

Flux Distribution under: (b) No Load; (d) Half Load; (f) Full Load

The field and flux distribution plots in air-gap for no load, half load and full load conditions for the case of faulty motor with 10% short are shown in Fig. 6. The plots with 20% short are shown in Fig. 7. From these figures, it can be observed that the

amplitudes of flux function and flux density decrease when the percentage of shorted turns increases. Also, when the load increases from no load to full load condition, a drastic increase can be found. These values are tabulated in Table II and the percentage change is also presented.

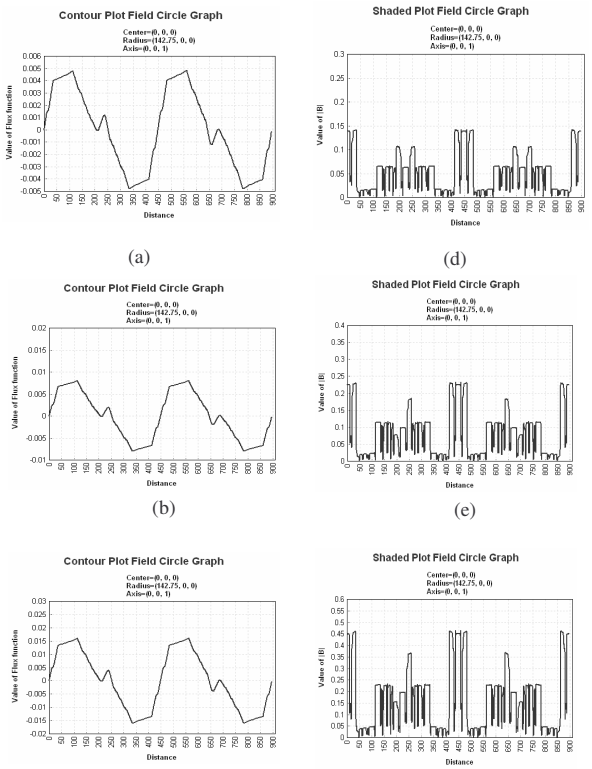

Fig. 6 Field and Flux Distribution in Air-Gap under 10% Inter-Turn Fault Conditions

Field Distribution under: (a) No Load; (c) Half Load; (e) Full Load

Flux Distribution under: (b) No Load; (d) Half Load; (f) Full Load

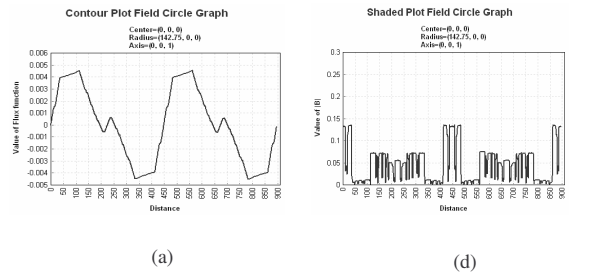

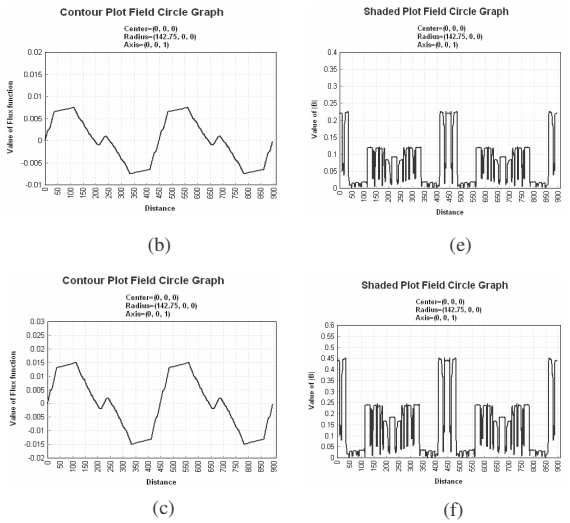

Fig. 7 Field and Flux Distribution in Air-Gap under 20% Inter-Turn Fault Conditions

Field Distribution under: (a) No Load; (c) Half Load; (e) Full Load

Flux Distribution under: (b) No Load; (d) Half Load; (f) Full Load

Table 2. Field analysis in air-gap

Condition		Flux Function (Wb)	Flux Density B, Wb/m^2	Percentage Change (%)	
				Flux Function	*Flux Density*
No Load	Normal	0.00506	0.14213	-	-
	10% Fault	0.00482	0.13962	4.73	1.76
	20% Fault	0.00453	0.13629	10.4	4.10
Half Load	Normal	0.00843	0.23479	-	-
	10% Fault	0.00798	0.23255	5.31	0.95
	20% Fault	0.00750	0.22700	11.0	3.31
Full Load	Normal	0.01686	0.47378	-	-
	10% Fault	0.01597	0.46509	5.32	1.83
	20% Fault	0.01500	0.45398	11.0	4.17
125% Load	Normal	0.02108	0.59418	-	-
	10% Fault	0.01996	0.58135	5.33	2.16
	20% Fault	0.01875	0.56747	11.0	4.49
150% Load	Normal	0.02528	0.70139	-	-
	10% Fault	0.02393	0.69628	5.35	0.73
	20% Fault	0.02250	0.68051	10.9	2.98

Table 2 shows the comparison results observed in air-gap. The change in percentage for flux function in 10% inter-turn short is around 5%, in 20% inter-turn short is around 11%.The percentage change for flux density in 10% inter-turn short is around 1% and in

20% inter-turn short is around 4%. From the above analysis, the flux function and flux density shows a gradual decrease when the turn-to-turn short increases.

5. Transient Analysis

Failure of nonadjacent bars is common in large cage induction motors. Since cage rotors of these machines are cylindrical, their symmetry and the presence of unavoidable manufacturing imperfections mean that there is the same probability of bar breakage occurring randomly anywhere in the cage. Consequently, progressive damage in the rotor could start simultaneously at different points of cage and then evolve from each point at a different speed, depending on the thermal, magnetic and dielectric asymmetries of the machine.

A. Induction Motor Model

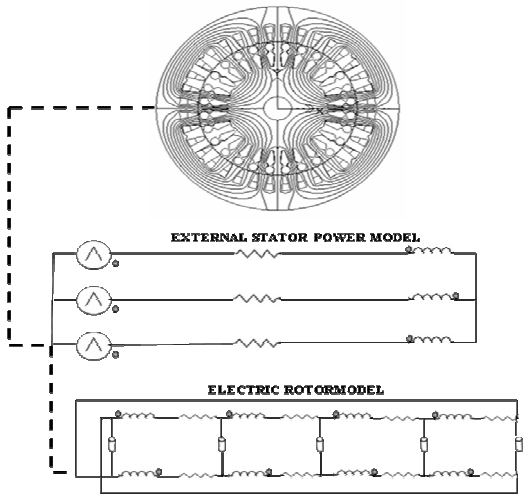

Fig. 8. Induction Motor Model

The electrical model representation of three phase squirrel cage star connected induction motor is shown in Fig. 8. The power source is considered as a voltage source connected with the series resistances and inductances of the stator windings in each phase. The rotor circuit model is made of short-circuited bar conductors. The circuit model of the three phase induction motor is shown in Fig. 9.

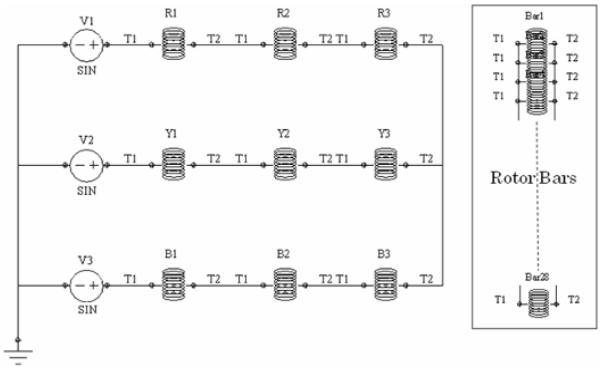

Fig. 9. Circuit Diagram of Induction Motor

B. Induction Motor Analysis

The stator is excited by a three phase AC supply and the rotor starts to rotate due to the torque developed and accelerates. The induced e.m.f. circulates current in the rotor and the motor is operated on full load condition. The self and mutual inductances are calculated from the flux linkages of the coil and the current through it.

The relative speed at the time of starting is, maximum and hence large e.m.f. is induced in the rotor conductors due to which very high current flows in the rotor which is generally five to seven times the full load current whereas the starting current in the stator will be eight to ten times the rated current. The stator phase current plots for the healthy and faulty conditions with 10%, 20% and 30% inter-turn faults are shown in Fig. 10 and Fig. 11. The time step is fixed as 10 ms.

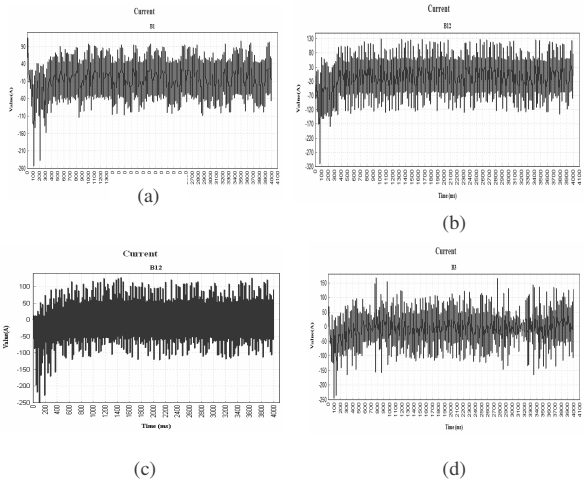

Fig. 10 Current Plots for Normal and Fault Conditions under Full Load:
(a) Healthy; (b) 10% Inter-turn;
(c) 20% Inter-turn; (d) 30% Inter-turn

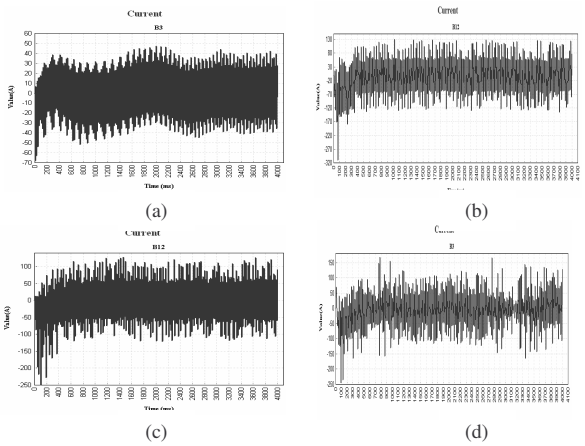

(a) (b) (c) (d)

Fig. 11 Current Plots for Normal and Fault Conditions under No Load:
(a) Healthy; (b) 10% Inter-turn;
(c) 20% Inter-turn; (d) 30% Inter-turn

From Table 3, it can be observed that the value of current increases when the percentage of inter-turn shorts increases, i.e., under the healthy motor condition, the current obtained is 56 A and under 10% inter-turn short condition, the current obtained is 77 A. Further, when the turn-to-turn short increases to 30%, the current obtained is 127 A. The percentage change in current for 10% inter-turn short is 27%, for 20% inter-turn short is 38% and for 30% inter-turn short is 56%, this observation shows an increase in the percentage change when the turn-to-turn short increases.

Table 3 Current analysis

	Condition	Current (A)	Percentage change (%)
No load	Normal	27	-
	10% Inter-Turn Short	32	15.63
	20% Inter-Turn Short	34	20.59
	30% Inter-Turn Short	40	32.50
Full load	Normal	56	-
	10% Inter-Turn Short	77	27.27
	20% Inter-Turn Short	90	37.78
	30% Inter-Turn Short	127	55.91

The torque produced in an induction motor depends on the part of the rotating magnetic field which reacts with the rotor, the magnitude of rotor current in running condition and the power factor of the rotor circuit in running condition. Therefore, the torque developed is directly proportional to flux and current.

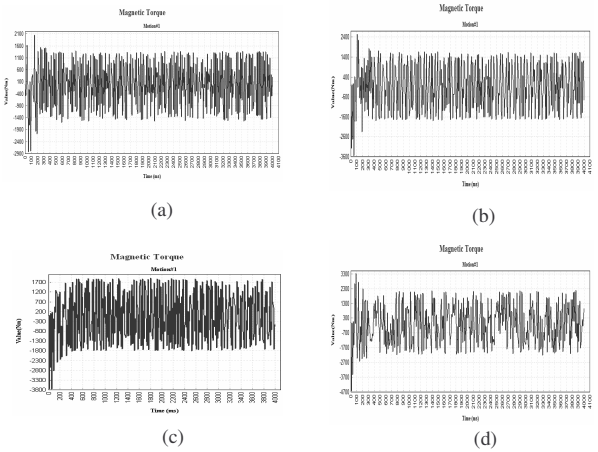

(a) (b) (c) (d)

Fig. 12. Magnetic Torque Plots for Normal and Fault Conditions under Full Load:
(a) Healthy; (b) 10% Inter-turn;
(c) 20% Inter-turn; (d) 30% Inter-turn

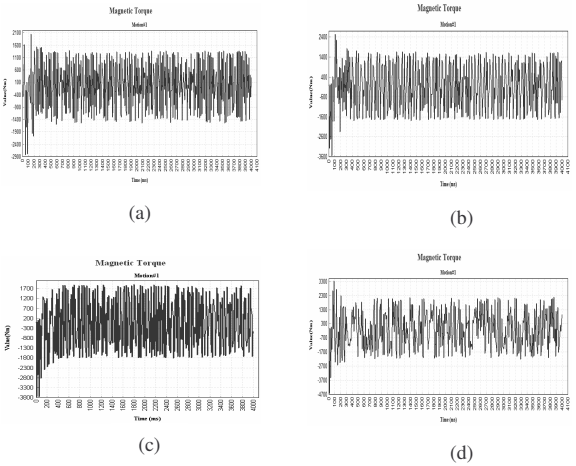

(a) (b) (c) (d)

Fig. 13. Magnetic Torque Plots for Normal and Fault Conditions under No Load:
(a) Healthy; (b) 10% Inter-turn;
(c) 20% Inter-turn; (d) 30% Inter-turn

The magnetic torque plots for the healthy and faulty conditions with two, four and eight broken bars are shown in Fig. 12 and Fig. 13. The time step is fixed as 10 ms. High torque is observed at the

starting and then decreases with further increase in time.

Table 4 Motor torque analysis

Condition		Magnetic Torque (Nm)	Percentage Change (%)
No Load	Normal	51	-
	10% Inter-Turn Short	73	30.14
	20% Inter-Turn Short	79	35.44
	30% Inter-Turn Short	87	41.38
Full Load	Normal	294	-
	10% Inter-Turn Short	476	38.24
	20% Inter-Turn Short	743	60.43
	30% Inter-Turn Short	930	68.39

From Table 4, it can be observed that the motor torque increases when the percentage of inter-turn shorts increases, i.e., under the healthy motor condition, the torque obtained is 294 Nm and under 10% inter-turn short condition, the torque obtained is 476 Nm. Further, when the turn-to-turn short increases to 30%, the torque obtained is 930 Nm. The percentage change in torque for 10% inter-turn short is 38%, for 20% inter-turn short is 60% and for 30% inter-turn short is 68%, this observation shows an increase in the percentage change when the turn-to-turn short increases.

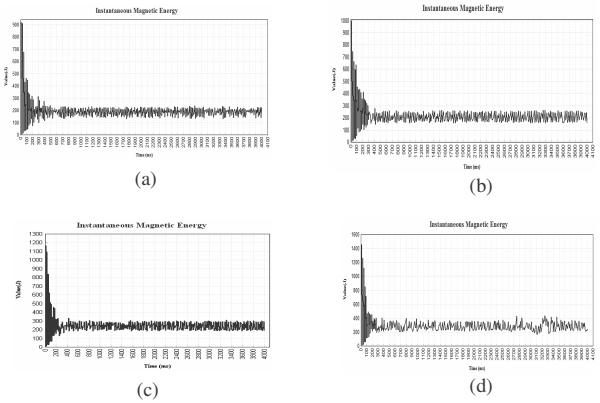

(a) (b) (c) (d)

Fig. 14. Instantaneous Magnetic Energy Plots for Normal and Fault Conditions under Full Load:
(a) Healthy; (b) 10% Inter-turn;
(c) 20% Inter-turn; (d) 30% Inter-turn

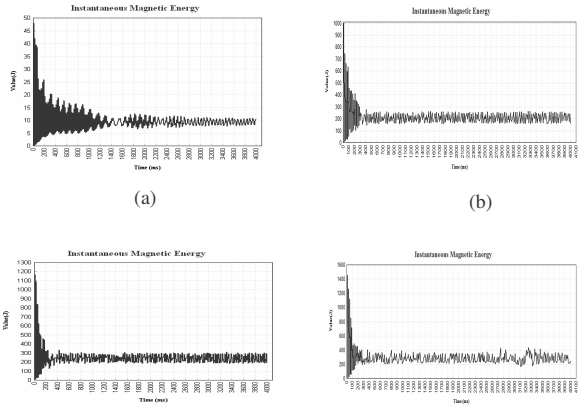

(a) (b) (c) (d)

Fig. 15. Instantaneous Magnetic Energy Plots for Normal and Fault Conditions under No Load:
(a) Healthy; (b) 10% Inter-turn;
(c) 20% Inter-turn; (d) 30% Inter-turn

When electric current flows in an inductor, energy is stored in the magnetic field. The instantaneous magnetic energy plots for the healthy and faulty conditions with two, four and eight broken bars are shown in Fig. 14 and Fig. 15. The time step is fixed as 10 ms. The instantaneous energy at the starting instant is found to be high and gradually decreases to attain a steady value when the time is increased to 4000 ms.

Table 5. Instantaneous magnetic energy analysis

Condition		Instantaneous magnetic energy (joules)	Percentage change (%)
No load	Normal	17	-
	10% inter-turn short	16	5.88
	20% inter-turn short	14	17.65
	30% inter-turn short	10	41.18
Full load	Normal	223	-
	10% inter-turn short	192	13.90
	20% inter-turn short	162	27.35
	30% inter-turn short	124	44.39

From Table 5, it can be observed that the instantaneous magnetic energy decreases when the percentage of inter-turn shorts increases, i.e., under the healthy motor condition, the energy obtained is

223 Joules and under 10% inter-turn short condition, the energy obtained is 192 Joules. Further, when the turn-to-turn short increases to 30%, the energy obtained is 124 Joules. The percentage change in energy for 10% inter-turn short is 14%, for 20% inter-turn short is 27% and for 30% inter-turn short is 44%, this observation shows an increase in the percentage change when the turn-to-turn short increases.

6. Conclusion

A three phase squirrel cage induction motor was modeled on the basis of finite element method. The simulation results were obtained for stator inter-turn faults. Comparisons were made between faulty and healthy motor and the results are given.

In the case of turn-to-turn faults, the flux distribution in the air-gap becomes non-uniform. The stored magnetic energy decreases when the percentage of fault in the stator increases. The flux function and the flux density also showed similar decreasing pattern when the percentage of fault was increased. The amplitude of the waveforms show drastic increase when the loads are increased. The flow of current in the stator phases and the torque produced in the motor also increases. The simulated results for magnetic energy, current, torque, flux function and flux density are presented.

References

1. Balamurugan S., Arumugam R., Paramasivam S., Malaiappan M. (2004) 'Transient Analysis of induction Motor Using Finite Element Analysis', IEEE Industrial Electronics Society, 30th annual conference, pp. 1526-1529.
2. Bangura J. F. and Demerdash N. A. (1999) 'Diagnosis and Characterization of Effects of Broken Bars and Connectors in Squirrel-Cage Induction Motor by Time-Stepping Coupled Finite Element State Space Modeling Approach', IEEE Trans. Electromagn. Compat., Vol. 14, No. 4, pp. 1167-1176.
3. Bentounsi A. and Nicolas A. (1998) 'On Line Diagnosis of Defaults on Squirrel Cage Motor Using FEM', IEEE Trans. Magn., Vol. 34, No. 5, pp. 3511-3574.
4. Bianchi N., Bolognani S., Comelato G. (1999) 'Finite Element Analysis of Three Phase Induction Motors: Comparison of Two Different Approaches', IEEE Trans. On Energy Conversion, Vol. 14, No. 4, pp. 1523-1528.
5. Elkasabgy N. M. and Eastham A. R. (1992) 'Detection of Broken Bars in the Cage Rotor on an Induction Machine', IEEE Trans. Ind. Appl., Vol. 28, No. 1, pp. 165-171.
6. Genadi Y. Sizov, Ahmed Sayed-Ahmed, nabeel (2009) 'Analysis and Diagnostics of Adjacent and Nonadjacent Broken-Rotor-Bar Faults in Squirrel-Cage Induction Machines', IEEE Trans. On Industrial Electronics, Vol. 56, No.11, pp. 4627-4641.
7. James L. Kirtley Jr., 'Designing Squirrel Cage Rotor Slots with High conductivity', Massachusetts Institute of Technology Cambridge.
8. John F. Watson, Neil C. Paterson, David G. Dorrell (1999) 'The Use of Finite Element Methods to Improve Techniques for the Early Detection of Faults in 3-Phase Induction Motors', IEEE Trans. On Energy Conversion, Vol. 14, No. 3, pp. 655-660.
9. Li Weili, XieYing, Shen Jiafeng, Luo Yingli (2007) 'Finite Element Analysis of Field Distribution and Characteristic Performance of Squirrel-Cage Induction Motor with Broken Bars', IEEE Trans. On Magnetics, Vol. 43, No. 4, pp. 1537-1540.
10. Martin Riera-Guasp, Man´es Fern´andez Cabanas, Jose A. Antonino-Daviu, Manuel Pineda-S´anchez (2010) 'Influence of Nonconsecutive Bar Breakages in Motor Current Signature Analysis for the Diagnosis of Rotor Faults in Induction Motors', IEEE transactions on energy conversion, vol. 25, no. 1.
11. Martin Riera-Guasp, Man´es Fern´andez Cabanas, Jose A. Antonino-Daviu, Pilar Molina Palomares (2008) 'The Use of the Wavelet Approximation Signal as a Tool for the Diagnosis of Rotor Bar Failures', IEEE transactions on Industry Applications, vol. 44, no. 3, pp. 716-726.
12. Mirafzal B. and Demerdash N. A. O. (2004) 'Induction Machine Broken-Bar Fault Diagnosis Using the Rotor Magnetic Field Space-Vector Orientation', IEEE Trans. Ind. Appl., Vol. 40, No. 2, pp. 534-542.
13. Preston T. W., Reece A. B. J., Sangha P. S. (1988) 'Induction Motor Analysis by Time-Stepping Techniques', IEEE Trans. on Magnetics, Vol. 24, No. 1, pp. 471-474.
14. Vaseghi B., Takorabet N., Meibody-Tabar F. (2008) 'Modeling of 1M with Stator Winding Inter-turn Fault Validated by FEM', Proceedings of the 2008 International Conference on Electrical Machines.
15. Williamson S., Robinson M. J. (1991) 'Calculation of Cage Induction Motor Equivalent Circuit Parameters using Finite Elements', IEEE Proc., Vol. 138, No. 5, pp. 264-276.
16. Aileen Christina. J, Nagarajan. S, S. Rama Reddy (2011) 'Detection of Broken Bars in Three Phase Squirrel Cage Induction Motor using Finite Element Method', 2011 *International Conference* on Emerging Trends in Electrical and Computer Technology, pp. 249-254.

Authors' information

S. Nagarajan received his B.E. degree in Electrical & Electronics Engineering from Sapthagiri College of Engineering, Chennai, India in 1998, M.E. degree in Power System from Anna University, Chennai, India in 2005. He has 12 years of teaching experience. He is presently a research scholar in Electrical and Electronics Engineering Department, Jerusalem College of Engineering, Collaborative Research Centre with Anna University, Chennai. His research interest is on the condition monitoring of 3-phase squirrel cage induction motor.

S.Rama Reddy is a professor in Electrical & Electronics Engg. Department, Jerusalem College of Engineering, Chennai, India. He obtained his M.E. in Power Systems from Anna University, Chennai and Ph.D in the area of Power Electronics from Anna University, Chennai, India. He has published 40 technical papers in national and international conferences proceedings / journals. He has worked in Tata Consulting Engineers, Bangalore and Anna University, Chennai. He has 18 years of teaching experience. His research interests include the areas of resonant converters and FACTS. He is life member of Institution of Engineers (India), Indian Society for Technical Education, Systems Society of India, Society of Power Engineers and Institution of Electronics and Telecommunication Engineers (India). He has published text books on Power Electronics, Solid State Circuits and Electronic Circuits.